*Regular Article*

# A Novel Multi-Dimensional Spectrum Estimation Technique using Antenna Array Displacement

**Viet-Ha Pham[1], Dominic Grenier[2], Jean-Yves Chouinard[2]**

[1] Dept. Electrical and Computer Engineering, the University of Western Ontario, London, ON, Canada
[2] Dept. Electrical and Computer Engineering, Université Laval, Québec, QC, Canada

Correspondence: Viet-Ha Pham, phamviet@gel.ulaval.ca

Manuscript communication: received 20 September 2011, accepted 10 November 2011

*Abstract*– **Conventionally, in multi-dimensional spectral estimation techniques, each data snapshot in space is captured simultaneously. All antenna elements or sensors being used to collect data are sampled at the same time. By doing so, the size of the antenna array is proportional to the area of interest in space. The antenna array is prohibitively huge if the area that we want to cover is large. In this paper, in order to reduce the number of antenna elements in use, we propose a novel multi-dimensional spectrum estimation technique based on displacing small antenna arrays along predefined paths. It includes a data measurement technique which sequentially collects data samples within each snapshot in space according to a predefined order, and a spectral estimation technique which is based on the Discrete Fourier Transform (DFT) of the collected data. The key idea is to create a large synthetic antenna aperture by displacing a small antenna array along a predefined trajectory. Impinging waves are assumed uniform plane waves. The performance of the proposed technique is evaluated by simulation. The applications of the proposed technique include synthetic aperture radar, radar image processing and sonar systems.**

*Keywords*– **Multi-dimensional spectral estimation, spatial sampling, wave vector spectrum estimation, uniform plan wave propagation.**

## 1 Introduction

Multi-dimensional spectral estimation found applications in many areas, such as sonar, radar, satellite imaging, radioastronomy, geophysics, and telecommunications [1–5]. Multi-dimensional signals are represented in the space and time domains while multidimensional spectra are represented in the wave vector and frequency domains [6, 7]. Similar to unidimensional spectral estimations, multidimensional spectrum estimation is also a classical and well-established research topic [8–13]. However, realization and implementation of multi-dimensional spectrum estimation technique in large-scale systems are still facing several challenges. One fundamental challenge is the prohibitively large size of the antenna systems being used to collect multi-dimensional data in space and time. Conventionally, the multi-dimensional spectrum in the wave vector and frequency domains is estimated by applying DFT on the signals collected in the space and time domains with the assumption that data samples on all antenna elements are collected simultaneously in the time domain. In this case, a large number of antenna elements or sensors is needed to cover a large area in space. In order to implement multi-dimensional spectral estimation technique, the number of required antenna elements needs to be reduced.

In this paper, we present a simple and novel multi-dimensional spectrum estimation technique based on creation of a large synthetic antenna aperture by displacing a small antenna array along a predefined path. The proposed technique includes a data collection technique and a spectrum calculation algorithm. In the data collection technique, the spatial signal samples are not collected simultaneously but sequentially along a predetermined path, e.g., along the $x$ axis. The spectrum calculation algorithm is based on the Discrete Fourier Transform (DFT) and a wave vector calibration procedure which is used to match the estimated spectrum peaks to the corresponding wave vectors. Simulation results show that the estimated wave vector spectrum matches closely the generated signal spectrum. The inaccuracies and limitations of the proposed methods are also discussed in this paper.

The paper is organized as follows. The discrete multi-dimensional Fourier Transform is described in Section 2. The proposed measurement technique is presented in Section 3. The spectrum estimation method and the wave vector calibration algorithm are presented in Section 4. Section 5 presents the simulation results for performance evaluation purpose. Section 6 concludes the paper.

## 2 Discrete Multidimensional Fourier Transform

Multi-dimensional Fourier Transform is used to calculate the wave vector spectrum of a signal in the spatial domain in a uniform plane wave propagation environment. A location in the three-dimensional (3D)

space is represented by a location vector $\vec{r}$ having coordinates $(r_x, r_y, r_z)$. The signals in the space and time domains are first sampled simultaneously in space at $(N_x \times N_y \times N_z)$ locations where $N_x$ is the number of sampling points in $r_x$ along the $x$ axis, $N_y$ is the number of samples in $r_y$ (on the $y$ axis), and $N_z$ is the number of points in $r_z$ ($z$ axis). The sampling steps in the $x$ axis is $\Delta r_x$ meters, $\Delta r_y$ meters in the $y$ axis, and $\Delta r_z$ meters in the $z$ axis. In the time domain, the signal is sampled at a sampling time interval of $\Delta t$ seconds or, equivalently at a sampling frequency of $\frac{1}{\Delta t}$ samples per second. Therefore, the discrete space-time signal is represented by a set of $N_x \times N_y \times N_z \times N_t$ samples where $N_t$ is the number of samples collected in time at each location in the space domain. At each sampling instant, a set of $N_x \times N_y \times N_z$ samples is collected in the space domain. At each sampling location, a set of $N_t$ samples is collected in the time domain.

In the wave vector domain, the discrete time-varying wave vector spectrum is also represented by a $(N_x \times N_y \times N_z \times N_t)$ matrix where $N_x$, $N_y$, and $N_z$ are the number of samples along the $k_x$, $k_y$, and $k_z$ axis in the wave vector domain, respectively, and $N_t$ is the number of samples in the time domain. The time-varying wave vector spectrum is obtained by applying the 3D DFT on each signal snapshot among $N_t$ snapshots in space and at $N_t$ discrete time instants. This relationship is expressed as follow [1, 2]:

$$S(\vec{k}_{m,n,l}, t) = \sum_{p=1}^{N_x} \sum_{q=1}^{N_y} \sum_{r=1}^{N_z} s(\vec{r}_{p,q,r}, t) e^{j\vec{r}_{p,q,r} \cdot \vec{k}_{m,n,l}} \quad (1)$$

$$s(\vec{r}_{p,q,r}, t) = \frac{1}{(2\pi)^3} \sum_{m=1}^{N_x} \sum_{n=1}^{N_y} \sum_{l=1}^{N_z} S(\vec{k}_{m,n,l}, t) e^{-j\vec{k}_{m,n,l} \cdot \vec{r}_{p,q,r}} \quad (2)$$

where $p$, $q$ and $r$ are the discrete indexes of $r_x$, $r_y$ and $r_z$ space vector components; $m$, $n$ and $l$ are the discrete indexes in the $k_x$, $k_y$ and $k_z$ wave vector components, respectively; and $t$ is the time variable. The sampling steps in $k_x$, $k_y$ and $k_z$ are $\Delta k_x$, $\Delta k_y$ and $\Delta k_z$. The relationships between the sampling steps in the wave vector domain and the sampling steps in the space domain are:

$$\Delta k_x = \frac{2\pi}{N_x \Delta r_x}, \quad \Delta k_y = \frac{2\pi}{N_y \Delta r_y}, \quad \Delta k_z = \frac{2\pi}{N_z \Delta r_z}. \quad (3)$$

The 3D DFT presented in Eq. (1) and (2), and the relationship presented in Eq. (3) are valid for space-time signals of which samples in each spatial snapshot are collected simultaneously. In the following sections, we present our proposed signal measurement and processing techniques which do not require the data samples in each spatial snapshot to be collected simultaneously. By doing so, we do not need a large number of antenna elements to cover the whole area of interest. Spatial signals can be collected sequentially in the time domain by moving a small antenna array along a predefined trajectory.

## 3 Proposed Measurement Technique in the Space-Time Domain

In our proposed measurement technique, the sampling locations are not sampled simultaneously but in a predefined order. The measurement site is discretized by $(N_x \times N_y \times N_z)$ locations in space. Denote **s** the space-time signal matrix and **p** the sampling location matrix. **s** is a $(N_x \times N_y \times N_z \times N_t)$ matrix containing signal samples collected in the space and time domains. **p** is a $(N_x \times N_y \times N_z)$ matrix representing the sampling locations in the space domain. In order to cover the whole area of interest of $(N_x \times N_y \times N_z)$ locations, we displace a rectangular antenna array of $(N_y \times N_z)$ elements along the $x$ axis. The antenna array plane is perpendicular to the $x$ axis and therefore is parallel to the $yz$ plane. The antenna elements are separated by $\Delta r_y$ and $\Delta r_z$ meters in the $y$ and $z$ axis, respectively. In the $x$ axis, the signal is sampled once every $\Delta r_x$ meters equivalently to once every $\Delta t$ seconds in the time domain. At the $k$th sampling instant, i.e., time instant $k\Delta t$, the $k$th lattice of the sampling location matrix **p**, i.e., the sampling locations with $r_x = k\Delta r_x$, is sampled.

After each period of $N_x \times \Delta t$ seconds, all the sampling locations are sampled. It is assumed that the signal wave vector spectrum is invariant during an estimation period. This assumption is reasonable because normally the antenna array size is not too big and the sampling period $\Delta t$ is small. After $N_p$ estimation periods, i.e., $N_p N_x \Delta t$ seconds, the number of collected samples is $N_p N_x N_y N_z$ samples. During the same time duration, the number of data samples collected by classical methods is $N_x N_y Nz \times N_p N_x$, which is $N_x$ times more than the data volume collected by our proposed measurement technique. More importantly, we replace the conventional $(N_x \times N_y \times N_z)$ antenna array by moving a $(N_y \times N_z)$ antenna array $N_x$ steps along the $x$ axis. This technique reduces the number of antenna elements and consequently reduces the antenna array manufacturing cost. It is also a solution to deploy huge antenna array systems.

Figure 1 shows an illustrative example of the proposed measurement technique. The example is presented for a two-dimensional (2D) space for simplicity. In this case, the rectangular antenna array reduces to a uniform linear antenna array. Antenna elements are separated by $\Delta r_y$ meters in the $y$ axis and are moved along the $x$ axis. The antennas in solid lines represent real antennas and the antennas in dot lines represent virtual antennas created by moving the real antenna array. The sampling distance in the $x$ axis is $\Delta r_x$ meters corresponding to $\Delta t$ seconds in the time domain. In the next section, we will present a spectrum estimation technique used for signals collected by the proposed measurement technique.

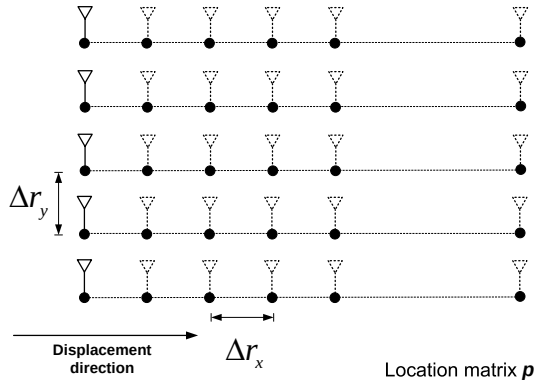


Figure 1. Virtual antenna array creation by displacement of a small antenna array along the $x$ axis in 2D space.

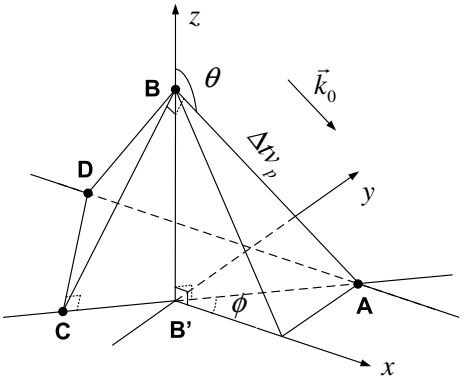


Figure 2. Transformation from rectangular sampling location matrix **p** to non-rectangular sampling location matrix **p′** and from non-rectangular sampling location matrix **p′** to rectangular sampling location matrix $\mathbf{p}^+$ in the 3D space domain.

## 4 Wave Vector Spectrum Estimation

In this section, we introduce the wave vector spectrum estimation technique, which operates on the data collected by the proposed measurement technique. For simplicity, we describe the spectrum estimation technique applied on the data collected during one estimation period of $N_x \times \Delta t$. The extension of the described spectrum estimation technique to the whole measurement duration is straightforward. In this case, signal matrix **s** is a $N_x \times N_y \times N_z$ matrix. Denote **S** the signal wave vector spectrum matrix. **S** is also a $N_x \times N_y \times N_z$ matrix. $\mathbf{s}(p,q,r)$ represents the space-time signal sample recorded at location vector $\vec{r} = (p\Delta r_x, q\Delta r_y, r\Delta r_z)$ and at time instant $p\Delta t$. $\mathbf{S}(m,n,l)$ is the spectrum component at wave vector $\vec{k} = (m\Delta k_x, n\Delta k_y, l\Delta k_z)$.

### 4.1 Spectrum Calculation

One observes that the relationship in Eq. (3) cannot be directly used to determine the sampling step $\Delta k_x$ in $k_x$ axis because the signal samples are not measured at the same time along the $x$ axis in the space domain. In this section we introduce a technique to transform the recorded signal matrix to space-time signal matrices which is sampled simultaneously in time. The relationship in Eq. (3) is applicable on these signal matrices.

Considering the spectrum component at wave vector $\vec{k_0}$, $\mathbf{S}(\vec{k_0})$, as illustrated in Figure 2. Point A is the sampling location $(p\Delta r_x, q\Delta r_y, r\Delta r_z)$ in the 3D space domain. In the time domain, the sample at point A is collected at instant $p\Delta t$. Assuming uniform plane wave propagation, the space-time signal component corresponding to the wave vector spectrum component $\mathbf{S}(\vec{k_0})$ at time instant $p\Delta t$ at point A is the delayed version of that component measured at time instant $(p-1)\Delta t$ at point B. The distance BA between the two points is $\Delta t v_p$ and vector $\vec{BA}$ points in the direction of wave vector $\vec{k_0}$. The coordinates of point B are $(p\Delta r_x - \Delta t v_p \sin\theta\cos\phi, q\Delta r_y - \Delta t v_p \sin\theta\sin\phi, r\Delta r_z - \Delta t v_p \cos\theta)$, where $\phi$ is the azimuthal angle from the $x$ axis to the projection of wave vector $\vec{k_0}$ in the $x-y$ plane, with $0 \le \phi \le 2\pi$, $\theta$ is the inclination angle from the $z$ axis to wave vector $\vec{k_0}$, with $0 \le \theta \le \pi$, and $v_p$ is the propagation velocity of electromagnetic waves in free space, i.e., $v_p = 3 \times 10^8$ m/s. Generalizing this process, we found that the space-time signal component corresponding to the wave vector spectrum component $\mathbf{S}(\vec{k_0})$ at time instant $p\Delta t$ at point A is the delayed version of that component measured at time instant $\Delta t$ at location:

$$\begin{aligned} &(p\Delta r_x - (p-1)\Delta t v_p \sin\theta\cos\phi, \\ &q\Delta r_y - (p-1)\Delta t v_p \sin\theta\sin\phi, \\ &r\Delta r_z - (p-1)\Delta t v_p \cos\theta) \end{aligned} \tag{4}$$

Repeating this step for all the sampling locations, the sampling location matrix **p**, for which the data samples are not recorded simultaneously, is transformed into location matrix **p′**, where all the data samples would be recorded simultaneously at time instant $\Delta t$. The sampling locations of matrix **p′** are represented in Eq. (4) with $p = 1,\ldots,N_x$, $q = 1,\ldots,N_y$, $r = 1,\ldots,N_z$. However, the transformed sampling location matrix, **p′**, is not rectangular and the spectrum estimation based on this sampling location set is not convenient: another transformation is required to transform matrix **p′** into a rectangular matrix.

Consider wave front $F_0$, corresponding to wave vector $\vec{k_0}$, at point B. Point D is the intersection of wave front $F_0$ and the line starting from point A and in parallel with axis $x$. Since the wave is assumed to be uniform and plane, the recorded signals at point B and at point D are identical. The coordinates of point D are $\left(p\Delta r_x - \Delta t v_p/(\sin\theta\cos\phi), q\Delta r_y, r\Delta r_z\right)$. Generalizing and repeating this transformation for all sampling locations and considering time instant $t = \Delta t$ as the time reference, the non-rectangular sampling location matrix **p′** in Eq. (4) is transformed to rectangular sampling location matrix $\mathbf{p}^+$. The locations of matrix $\mathbf{p}^+$ are sampled simultaneously at time instant $t = \Delta t$. The coordinates of locations in matrix $\mathbf{p}^+$ are:

$$\left(p\Delta r_x - (p-1)\Delta t v_p/(\sin\theta\cos\phi), q\Delta r_y, r\Delta r_z\right). \tag{5}$$

Matrix $\mathbf{p}^+$ is called the equivalent sampling location matrix of wave vector component $S(\vec{k_0})$. Two equivalent sampling location matrices are identical if the

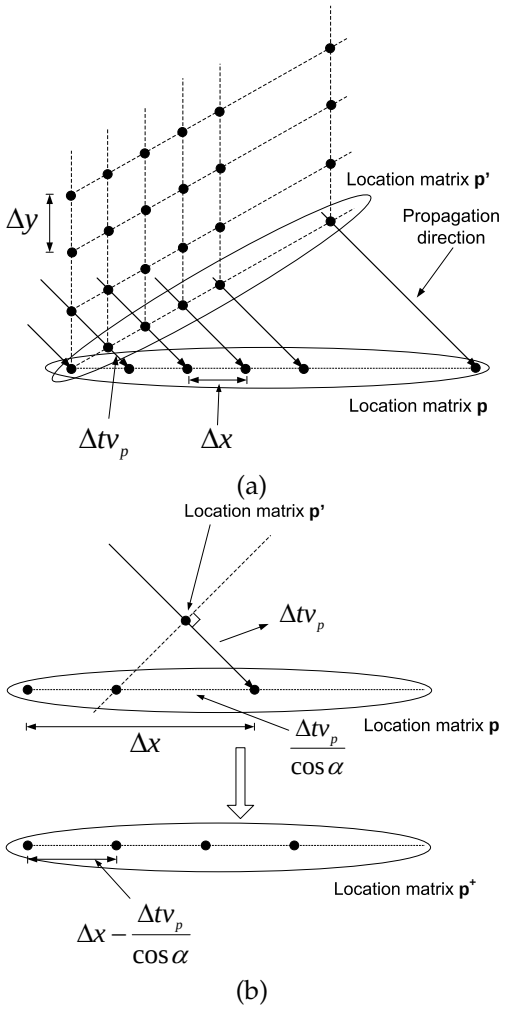


Figure 3. (a) Transformation from rectangular sampling location matrix **p** to non-rectangular sampling location matrix **p'** and (b) from non-rectangular sampling location matrix **p'** to rectangular sampling location matrix $\mathbf{p}^+$ in the 2D space domain.

corresponding wave vectors have the same propagation direction. Figure 3(a) illustrates the transformation from rectangular sampling location matrix **p** to non-rectangular sampling location matrix **p'**. Figure 3(b) illustrates the transformation from non-rectangular matrix **p'** to rectangular sampling location matrix $\mathbf{p}^+$. The illustration is presented in the 2D space domain for simplicity.

### 4.2 Wave Vector Calibration

Even if the sampling locations are explicitly expressed in Eq. (5) for wave vector spectrum component $\mathbf{S}(\vec{k_0})$, it is difficult to use this relationship to determine precisely the sampling steps in space, and therefore the sampling step in the wave vector domain, since wave vector $\vec{k_0}$ is unknown a priori. However, Eqs. (4) and (5) leads to a technique that determines the sampling steps in space domain, $\Delta r_x$, $\Delta r_y$ and $\Delta r_z$, and therefore the sampling steps in wave vector domain, $\Delta k_x$, $\Delta k_y$ and $\Delta k_z$, for any wave vector component $\mathbf{S}(\vec{k})$.

Applying the multidimensional discrete Fourier transform on the collected samples, i.e., on the signal matrix **s** in the spatial domain, one obtains a multidimensional matrix, called the spectrum matrix **S**. In order to obtain the wave vector spectrum of the signal, we need to determine the wave vector, or equivalently the sampling steps in wave vector, $\Delta k_x$, $\Delta k_y$ and $\Delta k_z$, for each spectrum component of the spectrum matrix **S**. Considering spectrum component $\mathbf{S}(m,n,l)$, the equivalent sampling steps in $r_y$, $r_z$ are $\Delta r_y$ and $\Delta r_z$, respectively, as the spatial signal is collected simultaneously in $y$ and $z$ axis in the space domain. The sampling steps along the wave vector axis $k_y$ and $k_z$ are calculated as per Eq. (3), i.e., $\Delta k_y = 2\pi / N_y \Delta r_y$ and $\Delta k_z = 2\pi / N_z \Delta r_z$. According to Eq. (5), the wave vector component $\mathbf{S}(m,n,l)$ is estimated with a sampling step of $\left|\Delta r_x - \Delta t v_p / (\sin\theta\cos\phi)\right|$ in the $x$ axis in the spatial domain. According to Eq. (3), the sampling step in the $k_x$ axis in the wave vector domain is:

$$\Delta k_x = \frac{2\pi}{N_x \left|\Delta r_x - \Delta t v_p / (\sin\theta\cos\phi)\right|} \tag{6}$$

From the definition of azimuthal and inclination angles, it is noted that:

$$\begin{cases} \cos\phi = \dfrac{m\Delta k_x}{\sqrt{(m\Delta k_x)^2 + (n\Delta k_y)^2}} \\ \sin\theta = \dfrac{\sqrt{(m\Delta k_x)^2 + (n\Delta k_y)^2}}{\sqrt{(m\Delta k_x)^2 + (n\Delta k_y)^2 + (l\Delta k_z)^2}} \end{cases} \tag{7}$$

In Eqs. (6) and (7), the only unknown is $\Delta k_x$. Analyzing these equations with assumption that $\Delta r_x - \Delta t v_p / (\sin\theta\cos\phi) < 0$ one obtains:

$$\left[\Delta r_x^2 - (\Delta t v_p)^2\right]\Delta k_x^2 + \frac{4\pi}{N_x}\Delta r_x \Delta k_x + \left(\frac{2\pi}{N_x}\right)^2 - \frac{(n\Delta k_y)^2 + (l\Delta k_z)^2}{m^2}(\Delta t v_p)^2 = 0 \tag{8}$$

Eq. (8) is of a quadratic form: $ax^2 + bx + c = 0$, where constants $a, b, c$ are given by:

$$\begin{cases} a = \Delta r_x^2 - (\Delta t v_p)^2 \\ b = \frac{4\pi}{N_x}\Delta r_x \\ c = \left(\frac{2\pi}{N_x}\right)^2 - \frac{(n\Delta k_y)^2 + (l\Delta k_z)^2}{m^2}(\Delta t v_p)^2 \end{cases} \tag{9}$$

Similarly, if $\Delta r_x - \Delta t v_p / (\sin\theta\cos\phi) > 0$, one obtains:

$$\left[\Delta r_x^2 - (\Delta t v_p)^2\right]\Delta k_x^2 - \frac{4\pi}{N_x}\Delta r_x \Delta k_x + \left(\frac{2\pi}{N_x}\right)^2 - \frac{(n\Delta k_y)^2 + (l\Delta k_z)^2}{m^2}(\Delta t v_p)^2 = 0 \tag{10}$$

Eq. (10) is of a quadratic form: $ax^2 - bx + c = 0$, where constants $a$, $b$ and $c$ are given in Eq. (9).

Once the solutions of Eq. (8) and Eq. (10) are found, the wave vector corresponding to spectrum element $\mathbf{S}(m,n,l)$ at wave vector $\vec{k} = (m\Delta k_x, n\Delta k_y, l\Delta k_z)$ is determined. The solution must be positive and satisfy the assumption on the sign of $\Delta r_x - \Delta t v_p / (\sin\theta\cos\phi)$. If $\Delta r_x - \Delta t v_p < 0$, then $\Delta r_x - \Delta t v_p / (\sin\theta\cos\phi) < 0$ and both solutions of Eq. (8), i.e., $(-b + \sqrt{\Delta})/2a$ and $(-b - \sqrt{\Delta})/2a$, where $\Delta = b^2 - 4ac$, could be

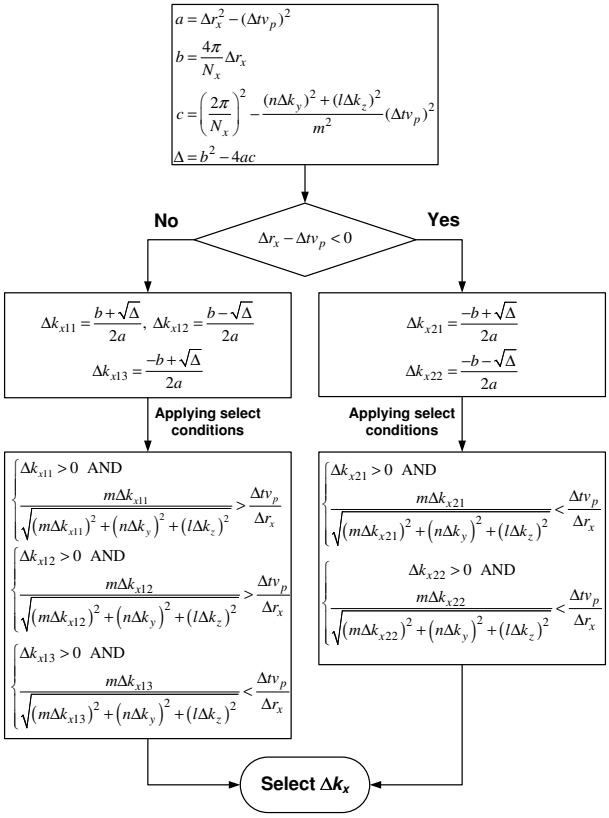


Figure 4. Wave vector calibration algorithm.

positive. In the other situation, if $\Delta r_x - \Delta t v_p > 0$, $\Delta r_x - \Delta t v_p / (\sin\theta \cos\phi)$ could be either negative or positive. In this case, both solutions of Eq. (10), i.e., $(b + \sqrt{\Delta})/2a$ and $(b - \sqrt{\Delta})/2a$, and the first solution of Eq. (8), i.e., $\frac{-b+\sqrt{\Delta}}{2a}$, could be positive. This technique is illustrated in Figure 4 and used in the simulation to estimate the signal wave vector spectrum.

## 5 Simulations results

In the previous sections, we have presented the proposed measurement technique in the 3D space domain and the spectrum estimation technique in the 3D wave vector domain. As it is difficult to represent graphically the spatial signal and the wave vector spectrum in 3D space and 3D wave vector domains, we present in this section simulation results in 2D space and 2D wave vector domains. In these simulations, the sampling period, $\Delta t$, is $T_s/8$, the sampling steps in the $x$ axis, $\Delta r_x$, and in the $y$ axis, $\Delta r_y$, are set to $\lambda/32$, where $T_s$ is the signal period and $\lambda$ is the signal wavelength. The considered signals are $\cos 2\pi f_0 t$, where the frequency $f_0$ is 800 MHz, propagating in different directions.

### 5.1 2-dimensional space and wave vector domains

Figure 5 shows a signal spectrum in the 2D wave vector domain. The signal in this example propagates along the direction of the $x$ axis. The spectrum is estimated by using a 2D discrete Fourier transform of $32 \times 32$ FFT points. Figure 5 shows the obtained

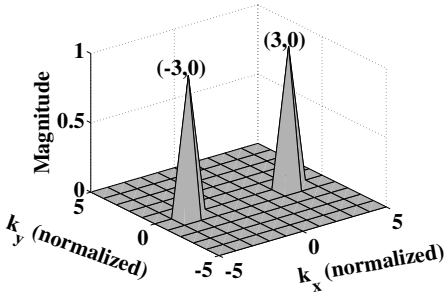


Figure 5. Signal spectrum in 2D wave vector domain: signal propagation direction is along the $x$ axis.

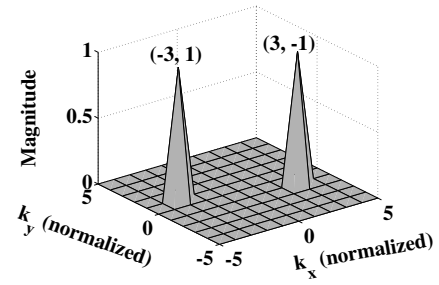


Figure 6. Signal spectrum in 2D wave vector domain: the angle between the signal propagation direction and the $x$ axis is $-\frac{\pi}{4}$.

spectrum matrix, **S**, with some arrangement so that we could observe the negative part of the wave vector spectrum. There are two peaks found at positions (-3,0) and (3,0). The pair $(x, y)$ refer to the element $\mathbf{S}(x, y)$ in spectrum matrix **S** since the wave vector calibration is not performed in this figure. Using the wave vector calibration technique, described in Section 4, the wave vector sampling steps, $\Delta k_x$ and $\Delta k_y$, at the two peaks are found at 5.59 rad/m and 16.76 rad/m, respectively. The two wave vectors corresponding to the two peaks are $(-16.76, 0)$ and $(16.76, 0)$. The magnitudes of these two wave vectors are 16.76 and the corresponding frequencies are 800 MHz. This means that there are two complex exponentials at a frequency of 800 MHz and propagating in the positive and negative directions of axis $x$. In this example, the estimated spectrum matches the expected spectrum.

Figure 6 shows the spectrum matrix of a cosine function, $\cos 2\pi f_0 t$, propagates in the direction of $\vec{k_0}$, of which the azimuthal angle is $-\frac{\pi}{4}$. One observes two peaks at positions $(-3, 1)$ and $(3, -1)$. Applying the wave vector calibration technique, the values of $\Delta k_x$ and $\Delta k_y$ at these two positions are found at 3.95 and 11.85, respectively. The wave vectors at the two peaks are $(-11.85, 11.85)$ and $(11.85, -11.85)$. Therefore the estimated spectrum consists of two wave vector impulses with the azimuthal angles of $\frac{3\pi}{4}$ and $-\frac{\pi}{4}$ and at frequencies of 800 MHz.

The signal under consideration in Figure 7 consists of three cosine functions at a frequency of 800 MHz, of which, one propagates in the direction of the $x$ axis, one propagates in the direction of $\frac{\pi}{6}$ or $30^o$ and one propagates in the direction of $-\frac{\pi}{3}$ or $-60^o$, with respect to the $x$ axis. The wave vector spectrum is estimated

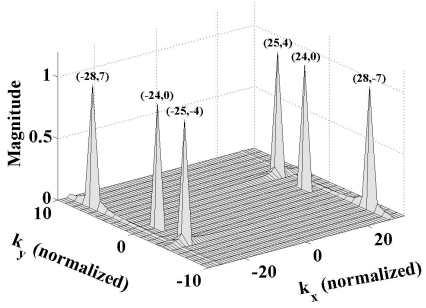


Figure 7. Signal spectrum in 2D wave vector domain; the angle between the signal propagation directions and the $x$ axis are 0, $\frac{\pi}{6}$ and $-\frac{\pi}{3}$.

by a 2D DFT of $256 \times 256$ FFT points. Figure 7 shows an enlargement of the spectrum matrix with $64 \times 20$ points around the wave vector origin. In this figure, there are six peaks at positions (-24,0) and (24,0), (-25,-4) and (25,4), (-28,7) and (28,-7). Using the proposed technique, the values of $\Delta k_x$ and $\Delta k_y$ at positions (-24,0) and (24,0) are 0.70 and 2.09, respectively. The wave vectors at these positions are (-16.76,0) and (16.76,0). These peaks correspond to two wave vector impulses propagating in the positive and negative directions of the $x$ axis at frequencies of 800 MHz. Similarly, at positions (-25,-4) and (25,4), the values of $\Delta k_x$ and $\Delta k_y$ are 0.58 and 2.09, respectively. The two wave vectors are (-14.45,-8.38) and (14.45,8.38). These peaks equal to two wave vector impulses propagating in the positive and negative directions of wave vector $\vec{k_1}$ that forms an angle of 30.10° with respect to axis $x$ and at frequencies of 797.48 MHz. At positions (-28,7) and (28,-7), the values of $\Delta k_x$ and $\Delta k_y$ are found at 0.28 and 2.09. The wave vectors at these positions are (-7.82,14.66) and (7.82,-14.66). These peaks correspond to two wave vector impulses that propagate in the positive and negative directions of wave vector $\vec{k_2}$ that form an angle of -61.93° with respect to axis $x$ and at frequency of 793.33 MHz.

### 5.2 Spectrum estimation accuracy

In the example of Figure 7, comparing the generated wave vector spectrum and the estimated wave vector spectrum, one found that there is inaccuracy with the spectrum components at wave vectors $\vec{k_1}$ and $\vec{k_2}$. At wave vector $\vec{k_1}$, there are errors of 2.52 MHz, or equivalently 0.32%, in frequency and 0.1°, or 0.33%, in azimuthal angle. At wave vector $\vec{k_2}$, there are errors of 6.67 MHz, or 0.83%, in frequency and 1.93°, or 3.22%, in azimuthal angle.

First, since there are three wave vector components at three different propagation directions, there are also three different equivalent sampling location matrices, $\mathbf{p}^+$. The measured space-time signal is equivalently the superposition of three wave vector spectrum components sampled simultaneously at time instant $\Delta t$ and at three different sampling location matrices. As the propagation direction spreads, the estimation precision degrades.

Second, the FFT resolution used in the wave vector spectrum estimation process is relatively low. Our tests show that an increase from $256 \times 256$ FFT points to $1024 \times 1024$ FFT points will improve the accuracy of about 50%.

Third, the equivalent spatial sampling step in $x$ axis, $\left|\Delta r_x - \Delta t v_p / \cos\alpha\right|$, is dependent on the propagation direction, $\alpha$. As mentioned above, the sampling period is $T_s/8$ while the sampling steps in the $x$ axis is $\lambda/32$. Therefore, $\Delta r_x - \Delta t v_p / \cos\alpha$ is negative. As the azimuthal angle of the wave vectors increase, the spatial sampling step in $x$ axis, $\left|\Delta r_x - \Delta t v_p / \cos\alpha\right|$, increases and thus, reduces the spatial resolution and the estimation accuracy. This is clearly observed in the example of Figure 7: as the azimuthal angle of wave vector $\vec{k_1}$ is smaller than the azimuthal angle of wave vector $\vec{k_2}$, the calibration accuracy at wave vector $\vec{k_1}$ is better than that at wave vector $\vec{k_2}$.

## 6 Conclusion

In order to estimate the wave vector spectrum of a spatial signal, the signal samples in each snapshot in space need to be collected simultaneously. This is not suitable for systems operating over a large area in the space since it requires a huge antenna array. In this paper, we present a measurement technique in which the spatial signal samples are not collected simultaneously but sequentially along a predefined path, e.g., in the direction of the $x$ axis, and a wave vector spectrum estimation technique which is based on the multidimensional Discrete Fourier Transform. A wave vector calibration algorithm is also presented in order to match the estimated spectrum peaks to the corresponding wave vectors. The key idea behind the proposed technique is the creation of a large virtual antenna array from a few of antenna elements by displacing the antenna array along a predefined path. The performance of the spectrum estimation technique is evaluated through a series of simulations in two-dimensional space and wave vector domains. The simulation results show that the estimated spectrum closely matches the generated wave vector spectrum with slight inaccuracies when the angle of arrival widely spreads. In practical situations, where high estimation accuracy is not the primary requirement but low antenna array implementation complexity and fast response are indeed required, the proposed measurement and spectrum estimation techniques can be used for beam detection and AoA estimation. The proposed techniques find applications in synthetic aperture radar (SAR), radar processing and sonar applications.

## Acknowledgements

This work was supported by the Fonds québécois de la recherche sur la nature et les technologies (FQRNT) under research team project grant PR-113970 and by the Natural Sciences and Engineering Research Council of Canada (NSERC) under discovery grant RGPIN 42906.

## References


[1] J. Capon, "High-resolution frequency-wavenumber spectrum analysis," *Proceedings of the IEEE*, vol. 57, no. 8, pp. 1408–1418, Aug. 1969.

[2] D. H. Johnson, "The application of spectral estimation methods to bearing estimation problems," *Proceedings of the IEEE*, vol. 70, no. 9, pp. 1018–1028, Sep. 1982.

[3] S. Lang and J. McClellan, "Spectral estimation for sensor arrays," *IEEE Transactions on Acoustics, Speech, and Signal Processing*, vol. 31, no. 2, pp. 349–358, Apr. 1983.

[4] R. Kumaresan and D. W. Tufts, "Estimating the angles of arrival of multiple plane waves," *IEEE Transactions on Aerospace and Electronic Systems*, no. 1, pp. 134–139, Jan. 1983.

[5] O. Santolík, F. Lefeuvre, M. Parrot, and J. L. Rauch, "Complete wave-vector directions of electromagnetic emissions: Application to INTERBALL-2 measurements in the nightside auroral zone," *Journal of Geophysical Research*, vol. 106, no. A7, pp. 13,191–13,201, 2001.

[6] G. D. Durgin, *Space-Time Wireless Channels*. Prentice Hall, 2002.

[7] P. Guguen and G. E. Zein, *Les Techniques Multi-Antennes pour les Réseaux Sans Fil*. Hermes Science, 2004.

[8] J. H. McClellan, "Multidimensional spectral estimation," *Proceedings of the IEEE*, vol. 70, no. 9, pp. 1029–1039, Sep. 1982.

[9] S. Lang and J. McClellan, "Multidimensional MEM spectral estimation," *IEEE Transactions on Acoustics, Speech, and Signal Processing*, vol. 30, no. 6, pp. 880–887, Dec. 1982.

[10] M. Wax, T.-J. Shan, and T. Kailath, "Spatio-temporal spectral analysis by eigenstructure methods," *IEEE Transactions on Acoustics, Speech, and Signal Processing*, vol. 32, no. 4, pp. 817–827, Aug. 1984.

[11] N. Srinivasa, K. Ramakrishnan, and K. Rajgopal, "Two-dimensional spectral estimation: A radon transform approach," *IEEE Journal of Oceanic Engineering*, vol. 12, no. 1, pp. 90–96, Jan. 1987.

[12] T. P. Bronez, "Spectral estimation of irregularly sampled multidimensional processes by generalized prolate spheroidal sequences," *IEEE Transactions on Acoustics, Speech, and Signal Processing*, vol. 36, no. 12, pp. 1862–1873, Dec. 1988.

[13] A. Hanssen, "Multidimensional multitaper spectral estimation," *Signal Processing*, vol. 58, no. 3, pp. 327–332, May 1997.


**Viet-Ha Pham** received the B.Sc.A., M.Sc., and Ph.D. degrees from Hanoi University of Technology, Hanoi, Vietnam; Pohang University of Science and Technology, Pohang, South Korea; and Laval University, Québec, QC, Canada, in 1997, 2003, and 2010. From Sep. 1997 to Aug. 2000, he is a lecturer at the Department of Computer Engineering, Hanoi University of Technology. He is currently a Postdoctoral Fellow at the Department of Electrical and Computer Engineering, University of Western Ontario, London, ON, Canada. His research interests include channel characterization and modeling, MIMO communications, channel prediction and adaptive transmission for broadband mobile wireless communications systems. He was a Technical Program Committee member for the 2008 IEEE ATC, 2010 IEEE VTC, 2011 IEEE ICC conferences and a reviewer for the IEEE Transactions on Broadcasting, IEEE Transactions on Vehicular Technology, IEEE Transactions on Signal Processing and IEEE Transactions on Wireless Communications. Dr. Pham is also an adjunct professor at Department of Computer Engineering, School of Information and Communications Technology, Hanoi University of Technology, Hanoi, Vietnam.

**Dominic Grenier** received the M.Sc. and Ph.D. degrees in electrical engineering in 1985 and 1989, respectively, from the Université Laval, Quebec City, Canada. From 1989 to 1990, he was a Postdoctoral Fellow in the radar division of the Defense Research Establishment in Ottawa (DREO), Canada. In 1990, he joined the Department of Electrical Engineering at Université Laval where he is currently a Full Professor. He was also co-editor for the Canadian Journal on Electrical and Computer Engineering during 6 years. Prof. Grenier is well recognized by undergraduate students in electrical and computer engineering. His excellence in teaching has resulted in his being awarded the "Best Teacher Award" many times. He obtained one special fellowship from the Quebec Minister for education in 2009; and the "Teaching Distinction Price" from Laval University in 2010. His research interests include inverse synthetic aperture radar imaging, statistical signal array processing for high resolution direction of arrivals and data fusion for identification. Prof. Grenier has 33 publications in refereed journals and 75 more in conference proceedings. In addition, 38 graduate students completed their thesis under his direction since 1992. Prof. Grenier is a registered professional engineer in the Province of Quebec (OIQ), Canada.

**Jean-Yves Chouinard** received the Ph.D. degrees from Laval University, Quebec city, Canada, in 1987. He was a Postdoctoral Fellow at the Space and Radio Communication Division, Center National d'Études des Télécommunications (CNET), Paris, France. From 1988 to 2002, J.-Y. Chouinard was a professor at the School of Information Technology and Engineering at the University of Ottawa. Since 2003 is with the Department of Electrical and Computer Engineering at Laval University. He is the author or co-author of more than 180 journal, conference papers and technical reports. He is a co-inventor for a US patent and has 2 more US patents pendings. His research interests are communications theory and applications, broadband wireless systems, and advanced broadcast technologies. He is co-recipient of the 1999 Neal Shepherd Best Propagation Paper Award from the IEEE Vehicular Society and the 2004 Signal Processing Best Paper Award from the European Journal of Signal Processing. He is a co-editor of a book on information theory and co-author book chapters on software reconfigurable MIMO wireless communication systems and on OFDM-based mobile broadcasting. He is a Technical Program Co-chair for the upcoming 2012 Vehicular Technology Conference (VTC'2012 Fall) in Quebec city. He is also a Director of the Canadian Society of Information Theory (CSIT). He is an Associate Editor for the IEEE Transactions on Broadcasting.